Fluxes and (co-)variances of reacting scalars in the convective boundary layer

By JEAN-FRANÇOIS VINUESA[1,2]* and JORDI VILÀ-GUERAU DE ARELLANO, [1]*Meteorology and Air Quality Section, Wageningen University, 6701 AP Wageningen, The Netherlands;* [2]*TNO-MEP, Postbus 342, 7300 AH Apeldoorn, The Netherlands*

ABSTRACT

The effects of chemistry on the transport and the mixing of reacting scalars in the convective atmospheric boundary layer (CBL) are investigated. To do this, we use large-eddy simulation (LES) to calculate explicitly the different terms of the flux and (co-)variance budget equations and to analyse in particular the role of the chemical term with respect to the thermodynamical terms. We examine a set of chemical cases that are representative of various turbulent reacting flows. The chemical scheme involves two reacting scalars undergoing a second-order reaction. In addition, we study a chemical cycle, based on a first- and a second-order reaction, to study the behaviour of chemical systems in equilibrium in turbulent flows. From the budget analysis, we found that the chemical terms become more relevant when the chemical timescale is similar to the turbulent timescale. In order to determine the importance of the chemical terms, we compared these terms to the dynamical terms of the budget equations. For the flux of reactants, the chemical term becomes the dominant sink in the bulk of the CBL. As a result, flux profiles of reacting scalars have non-linear shapes. For the covariance, which accounts for the segregation of species in the CBL, the chemical term can act as a sink or source term. Consequently, reacting scalar covariance profiles deviate considerably from the inert scalar profile. When the chemistry is in equilibrium, the chemical term becomes negligible and therefore the flux and (co-)variance profiles are similar to those of inert scalrs. On the basis of the previous budget results, we develop a parameterisation that represents the segregation of reacting species in large-scale models under convective conditions. The parameterisation is applied to an atmospheric chemical mechanism that accounts for ozone formation and depletion in the CBL. We found a good agreement between the parameterisation and the LES results.

1. Introduction

The chemical lifetime of reactants in the atmosphere can vary within a wide range of timescales. In the convective boundary layer (CBL), the so-called long-lived species are well mixed, and the vertical profile of their fluxes follow a linear shape (Wyngaard, 1985). For reactants with a short chemical lifetime or with a lifetime of the same order of magnitude as the turnover

time of the convective boundary layer, approximately 10–20 min, the chemical transformations can be limited by the turbulent mixing (Vilà-Guerau de Arellano and Lelieveld, 1998). This process influences the distribution of reacting scalars and the chemical composition of the CBL, and in particular the second-order moments of the concentration distributions, i.e. fluxes and (co-)variances. By including the chemical terms in the governing equations for reactants, one can study the relevance of accounting for these terms in fluxes and (co-)variances. When turbulence and chemistry have similar timescales, one would expect the chemical terms to make a contribution similar to that made by dynamical terms and, as a result, fluxes and

*Corresponding author address: Meteorology and Air Quality Section, Wageningen University, 6701 AP Wageningen, The Netherlands.
e-mail: vinuesa@hp1.met.wau.nl

(co-)variances will deviate from the inert linear profiles. Since these second-order moments, which describe the transport, the variability and the mixing of reacting scalars, are relevant for atmospheric chemistry, we intend to analyse the magnitude of these deviations. We perform this analysis using dimensionless numbers which depend on the CBL characteristics and chemical mechanisms.

Previous studies (Schumann, 1989; Sykes et al., 1994; Gao and Wesely, 1994; Verver et al., 1997; Molemaker and Vilà-Guerau de Arellano, 1998; Petersen et al., 1999; Petersen, 2000; Petersen and Holtslag, 1999; Krol et al., 2000; Patton et al., 2001) have shown that the turbulent mixing can control the concentration and the distribution of reacting scalars in the CBL. This influence is expressed mathematically by the chemical term included in the governing equations for the mean concentrations, for the fluxes and for the (co-)variances. Since reactant concentrations can be correlated or anti-correlated and since the chemical reaction rates depend on covariances, the way in which the species are mixed can have an important impact on the reaction rate (Schumann, 1989). A suitable variable to characterise this unmixed state of the reactants, and therefore the effect of inhomogeneous mixing on chemical transformations, is the intensity of segregation which can be defined as the ratio between the covariance and the product of the concentrations. There is a discussion concerning the importance of this variable in the atmospheric boundary layer. In a situation with uniform emissions, Krol et al. (2000) (from now, K2000) show relatively small segregation between reactants. However, Herwehe et al. (2000) found relevant differences in averaged mixing ratios when comparing the results obtained by large-eddy simulation (LES) and by a mesoscale model. In order to clarify these discrepant results, it is first necessary to determine the role played by the chemical terms in the flux and (co-)variance equations.

Although extensive studies on temperature, moisture and inert scalars have shown how the different dynamical terms contribute to the budget of fluxes and (co-)variances (Wyngaard et al., 1978; Lenschow et al., 1980; Moeng and Wyngaard, 1984; 1989), very few studies have addressed the second-order moment budgets of reacting scalars. To our knowledge, no study so far has presented the budget of reactant species in a CBL in a comprehensive manner.

In this paper, we analyse the effect of the chemical term on the transport and mixing of reacting scalars by decomposing flux and (co-)variance budget equations using LES. The simulations involve a species emitted at the surface, namely bottom-up scalar A, and a species entrained at the top of the CBL, namely top-down scalar B. We have simulated representative turbulent reacting flows in a CBL with a second-order irreversible reaction (i.e. A + B → C) and a chemical mechanism in equilibrium (i.e. A + B ⇌ C).

The structure of the paper is as follows. In section 2 we present the theoretical basis and the numerical simulation characteristics. The second-order moment budgets are analysed in sections 3–5. These analyses focus on the moderately fast chemical case, which is expected to be the one that is affected most by chemistry. A parameterisation of the effect of incomplete mixing on chemical transformations is developed in section 6. This parameterisation is based on the bottom-up top-down variance decomposition proposed by Moeng and Wyngaard (1984; 1989) and it is compared to the LES results. Moreover, the parameterisation is applied to a realistic atmospheric chemical scenario. Finally, the results are summarised in section 7.

2. Theoretical basis and numerical simulations

2.1. Theory

To increase readability, the horizontal averages are denoted by capital letters and the fluctuations of the variables around the horizontal average value by lower case letters. Since the turbulent fields under study are statistically invariant to translation of the horizontal axis, horizontal homogeneity of turbulence is assumed. Therefore, the vertical scalar flux budget equation reads

$$\frac{\partial \overline{ws_i}}{\partial t} = -\underbrace{\overline{w^2}\frac{\partial S_i}{\partial z}}_{G} + \underbrace{\frac{g}{\Theta_0}\overline{\theta s_i}}_{B} - \underbrace{\frac{\partial \overline{w^2 s_i}}{\partial z}}_{T} - \underbrace{\overline{s_i \frac{\partial \pi}{\partial z}}}_{P}$$
$$- \underbrace{\overline{s_i \frac{\partial \tau_{3j}}{\partial x_j}} - w\frac{\partial \langle s_i'' u_j'' \rangle}{\partial x_j}}_{D} + \underbrace{R_{\overline{ws_i}}}_{CH}, \qquad (1)$$

where w, θ and s_i represent the fluctuation of the vertical velocity, the temperature and the reactant concentration, respectively. Θ_0 is a reference state potential temperature, S_i is the horizontal average reactant quantity and π is the modified pressure defined as $[(p - p_0)/\rho_0] + (2/3)E$, where p, p_0 and ρ_0 are the pressure, a reference pressure and a reference

density respectively, and E is the subgrid-scale turbulent kinetic energy. The subgrid stress for momentum and scalar are represented by τ_{3j} and $\langle s_i'' u_j'' \rangle$, respectively. The terms on the right-hand side are the mean gradient term (G), the buoyancy (B), the turbulent transport (T), the pressure term (P), the dissipation (D) and the chemical contribution (CH).

Similarly, a general expression for the covariance budget of the resolved scale $\overline{s_i s_j}$ can be expressed as:

$$\frac{\partial \overline{s_i s_j}}{\partial t} = -\underbrace{\overline{ws_j}\frac{\partial S_i}{\partial z} - \overline{ws_i}\frac{\partial S_j}{\partial z}}_{G} - \underbrace{\frac{\partial \overline{ws_i s_j}}{\partial z}}_{T}$$
$$-\underbrace{\overline{s_j \frac{\partial \langle s_i'' u_k'' \rangle}{\partial x_k}} - \overline{s_i \frac{\partial \langle s_j'' u_k'' \rangle}{\partial x_k}}}_{D} + \underbrace{R_{\overline{s_i s_j}}}_{CH}. \quad (2)$$

The terms on the right-hand side are the gradient term (G), the turbulent transport (T) contributions, the dissipation at the sub-grid scale (D) and the chemical contribution (CH), respectively. Details of the variance budget equation will not be given here since this equation can be obtained by substituting i for j in the previous equation.

Considering a chemical cycle defined by:

$$\text{A} + \text{B} \overset{k}{\to} \text{C} \quad (3)$$

$$\text{C} \overset{j}{\to} \text{A} + \text{B}, \quad (4)$$

and focusing on reactant A, one can express the chemical terms of the previous budget equations as:

$$R_{\overline{wa}} = -k(\overline{wa}B + \overline{wb}A + \overline{wab}) + j\overline{wc}, \quad (5)$$

$$R_{\overline{a^2}} = -2k(\overline{a^2}B + \overline{ab}A + \overline{a^2 b}) + j\overline{ac}, \quad (6)$$

$$R_{\overline{ab}} = -k(\overline{ab}B + \overline{ab}A + \overline{a^2}B + \overline{b^2}A + \overline{a^2 b} + \overline{b^2 a})$$
$$+ j(\overline{ac} + \overline{bc}). \quad (7)$$

It is convenient to determine the order of magnitude of these chemical terms in eqs. (1) and (2) in order to show the relevance of accounting for these terms. Previous studies (Schumann, 1989; Sykes et al., 1994; Vilà-Guerau de Arellano and Lelieveld, 1998) have defined a reacting flows classification based on the Damköhler number (Da). This dimensionless number is the ratio of the flow timescale to the chemical

timescale. For the CBL and for the scalar A involved in a second-order reaction [i.e. reaction (3)], this number is defined as

$$Da_\text{A} = \frac{\tau_\text{t}}{\tau_\text{c}} = \frac{z_i}{w_*} k\langle B \rangle, \quad (8)$$

where τ_t and τ_c are the turbulent and the chemical timescales, respectively. $\langle B \rangle$ accounts for the bulk concentration of reacting scalar B. w_* is the the convective velocity scale defined by $[(g/\Theta_\text{v})\overline{w\theta_0}z_i]^{\frac{1}{3}}$ where g, Θ_v, $\overline{w\theta_0}$, z_i are the acceleration due to gravity, the virtual temperature, surface sensible heat flux and the CBL height, respectively. Well below its threshold value of 1 (i.e. $Da_\text{A} \ll 1$), the reacting flow can be considered as representative of a slow chemistry regime. In this case, the chemical transformation of reactants can be treated separately from the dynamics of the flow, since reacting scalars are homogeneously mixed by the turbulence. High above the threshold value (i.e. $Da_\text{A} \gg 1$), the chemical contribution to the scalar continuity equation becomes predominant and chemical species react in situ and are not transported; the flow is in fast chemistry regime. Between these extreme behaviors, e.g. for moderate chemistry, the turbulent mixing is expected to have a non-negligible impact on chemical transformations. In this case, all the terms of the governing equation for the reactant must be treated simultaneously.

In order to analyse the relevance of the chemical term related to the thermodynamical terms on the flux and (co-)variance, it is convenient to introduce dimensionless numbers that account for the chemical contribution to second-order moments. By defining the following characteristic scales of a turbulent reacting flow: the turbulent timescale (τ_t) and flux scales ($w_* s_{i*}$, $s_i = A$, B, C) as proposed by Cuijpers and Holtslag (1998), i.e.

$$w_* s_{i*} = \frac{1}{z_i} \int_0^{z_i} \overline{ws_i}\,\mathrm{d}z, \quad (9)$$

one can formulate the chemical term of the flux (5) and (co-)variances [eqs. (6) and (7)] in a dimensionless way. Notice that since inert scalar fluxes are linear in the CBL, only the surface flux and the entrainment flux are necessary to calculate the flux scales.

We derive as an example, the dimensionless expression for the chemical term (5) of the flux equation. Multiplying (5) by the turbulent timescale and dividing

by the velocity and concentration scales, we obtain:

$$\frac{1}{w_* a_*} \tau_t R_{\overline{wa}} = -\tau_t k \left(\frac{\overline{wa}}{w_* a_*} B + \frac{\overline{wb}}{w_* a_*} A + \frac{\overline{wab}}{w_* a_*} \right)$$
$$+ j\tau_t \frac{\overline{wc}}{w_* a_*}. \tag{10}$$

Following Petersen (2000), we have neglected the chemical third-order terms. Introducing now the dimensionless fluxes F_a, F_b and F_c and the Damköhler number defined by eq. (8), the dimensionless chemical term of the flux equation reads:

$$\frac{1}{w_* a_*} \tau_t R_{\overline{wa}} = -Da_A F_a - Da_B \frac{w_* b_*}{w_* a_*} F_b$$
$$+ Da_C \frac{w_* c_*}{w_* a_*} F_c. \tag{11}$$

Therefore an appropriate indicator of the importance of the chemical term contribution to the flux budget equation is the flux Damköhler number ($Da_{\overline{wa}}$), which is defined as

$$Da_{\overline{wa}} = \left| Da_A + Da_B \frac{w_* b_*}{w_* a_*} - Da_C \frac{w_* c_*}{w_* a_*} \right|. \tag{12}$$

Following a similar derivation, the corresponding dimensionless numbers for the (co-)variances read:

$$Da_{\overline{a^2}} = 2 \left| Da_A + Da_B \frac{a_* b_*}{a_*^2} - Da_C \frac{a_* c_*}{a_*^2} \right|, \tag{13}$$

$$Da_{\overline{ab}} = \left| Da_A + Da_B + Da_A \frac{a_*^2}{a_* b_*} + Da_B \frac{b_*^2}{a_* b_*} \right.$$
$$\left. - Da_C \frac{(a_* c_* + b_* c_*)}{a_* b_*} \right|, \tag{14}$$

where $Da_{\overline{a^2}}$ and $Da_{\overline{ab}}$ are called by analogy the (co-)variances Damköhler numbers. The Damköhler numbers for the species A, B and C with respect to the second-order reaction (3) for A and B and to the photolytic one (4) for C are Da_A, Da_B and Da_C, respectively. It is important to notice that $Da_{\overline{wa}}$, $Da_{\overline{a^2}}$ and $Da_{\overline{ab}}$ include explicitly the complete set of reactions in which the chemical species A is involved. For the average concentration equation of species A, the dimensionless chemical term is $|Da_A - Da_C(\langle C \rangle / \langle A \rangle)|$. The role of this term on the distribution and the evolution of the averaged concentration has been extensively discussed by K2000.

2.2. Numerical experiments

The model used is a three-dimensional LES code that Cuijpers and Duynkerke (1993), Siebesma and Cuijpers (1995) and Cuijpers and Holtslag (1998) described for the dynamics and Vilà-Guerau de Arellano and Cuijpers (2000) for the chemistry. We simulate an entraining CBL with a surface sensible heat flux of 0.052 Km s^{-1} and no latent heat flux. The geostrophic wind is chosen equal to zero and the initial potential temperature profile has a constant value of 288 K below 662.5 m and increases by 0.6 K every 100 m above 712.5 m. The prescribed grid has $64 \times 64 \times 60$ points in the horizontal and the vertical directions, representing a domain of 3.2 km $\times$ 3.2 km $\times$ 1.5 km. Periodic lateral boundary conditions are assumed. The maximum time-step used in the calculation is 0.5 s. For all the simulations, the convective velocity scale w_*, the CBL height z_i and the free convection timescale $t_* \equiv z_i / w_*$ are equal to 1.096 m s^{-1}, 747 m and 680 s, respectively after a pseudo-stationary steady state is reached ($\sim$1 h). The CBL height z_i is defined as the highest level at which the emitted scalar concentration exceed the threshold value of 0.005 ppb following the arguments discussed in Bretherton et al. (1999). The boundary layer depth obtained by using this method is about 10% higher than the one obtained by using the minimum heat flux. This different definition of z_i, however, does not affect the results.

Using the reacting flow classification described previously, we performed four numerical experiments: inert (I), moderately slow (MS), moderately fast (MF) and cycle (C). The simulations involve a bottom-up diffusive species (A) injected at the surface and a top-down species (B) which is entrained at the top of the CBL. The various chemical cases are defined using the reactions presented previously [(3) and (4)]. The scalar C is only produced by reaction (3) and depleted by reaction (4) (no initial concentrations; no emission or entrainment fluxes).

In the MS and MF experiments, the scalars A and B only undergo reaction (3), i.e. the photolytic rate constant is set at 0. The dimensionless reaction rate k, see Petersen (2000), of reaction (3) is 0.29 (4.75 $\times$ 10^{-3} ppb^{-1} s^{-1}) for all the simulations. In all the experiments, A is emitted at the surface with a surface flux of 0.1 ppbm s^{-1} with an initial concentrations in the CBL equal to 0. For these conditions, we obtained the following Damköhler numbers averaged over the second hour of simulation: $Da_A = 0.6$ for the MS experiment and $Da_A = 4.1$ for the MF one. For the MS,

the initial B concentration profile has a constant value of 0.5 ppb below 662.5 m and 2 ppb above this level; for the MF the values are equal to 1 and 10 ppb, respectively. Notice that the difference between moderately slow and fast chemistry is created by using different initial profiles and entrainment fluxes for B, i.e. by varying the volume concentration in the Damköhler numbers.

In addition, a cycle (chemical case C) composed of reactions (3) and (4) is studied in order to investigate the impact of the turbulent mixing on a chemical equilibrium. Reaction (4) represents a photolysis reaction with a dimensionless reaction rate of 29 (0.475 s^{-1}). As expected, the control parameter of a reacting scalar undergoing a chemical cycle is not equal to the individual Damköhler number as defined previously but it equals an overall Da as K2000 pointed out. This overall Da is the sum of individual Da weighted by the stoichiometric coefficient as it appears in the conservation equation for reacting scalars. For instance, here the individual Da is equal to 6.2 for reactant A, whereas the total Da, which includes all the production and destruction reactions, i.e. $|Da_A - Da_C(\langle C \rangle/\langle A \rangle)|$, is equal to 0.4.

Following the analysis used by Schumann (1989) and K2000, the sub-grid effects of the chemical terms are omitted. Here, we mainly present the results for the emitted reactant A. Nevertheless, similar results and conclusions can be drawn for the analysis of the entrained scalar B. The simulations cover a 2 h period, and the statistics presented here are obtained by averaging the results over the last hour of simulation. In the numerical experiments, the concentration of chemical species evolve with time. However, this evolution does not affect our results. Similar flux and (co-)variance profiles are found if one integrates for longer times. In addition, the results are scaled with the appropriate convective scaling parameters.

3. Scalar fluxes

Figure 1 shows the vertical profiles of scalar fluxes that consist of a resolved part and a sub-grid scale contribution modelled as a diffusion process. Notice that the concentration scale (i.e. c_{u*}) used to make the dimensionless profiles is calculated as the ratio of the emission flux of A to the convection velocity scale. Within the boundary layer, the profiles of inert scalars (temperature and bottom-up scalar for the inert chemical case) have a linear shape (Deardorff, 1979;
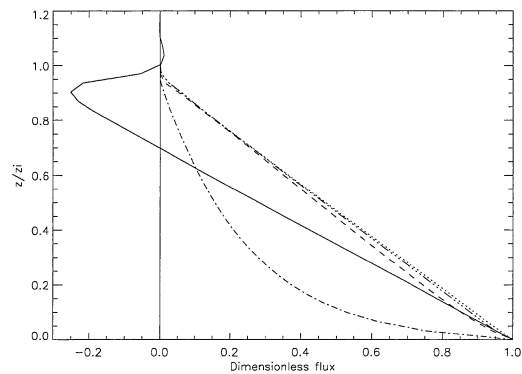

Fig. 1. Vertical profiles of the dimensionless fluxes for the bottom-up scalar A. The heat flux is represented by a solid line. The chemical fluxes for the various chemical cases are presented: Inert (dotted line), MS (dashed line), MF (dash dot line) and C experiments (dash dot dot dot line). The values are made dimensionless by $w_*\theta_*$ for the temperature and w_*c_{u*} for the chemical fluxes where w_*, θ_* and c_{u*} are the convection velocity scale, the temperature scale and the chemical scale for the bottom-up scalar respectively. The term c_{u*} is defined as the ratio of the surface flux of A to the convection velocity scale.

Wyngaard and Brost, 1984; Wyngaard, 1985). For reactive scalars, the profiles deviate from this shape. In fact, these deviations become more significant when the Damköhler number increases; they are larger for the MF experiment than for the MS. This was shown also by Gao and Wesely (1994), Sykes et al. (1994) and McDonald-Butler et al. (1999). These deviations are due to the fact that chemistry acts as a sink term in the flux budget. As the chemical contribution to fluxes increases with the reaction rate, the deviations will increase with the reaction rate and thus with the Damköhler numbers.

In order to quantify the degree to which chemistry is restricted by turbulence, it is appropriate to determine the turbulent Damköhler numbers (Da) and the flux Damköhler numbers (i.e. $Da_{\overline{ws}}$, see Table 1). In case C, the specific Damköhler numbers for each species are characteristics of fast chemistry ($Da_A = 6.2$, $Da_B = 2.3$ and $Da_C = 321$). However, the system is in a chemical equilibrium since the destruction of a chemical species by one reaction is balanced by the chemical production of the other one. In other words, the chemical term in the flux budget equation is composed of a sink and a source term. For a more complete chemical mechanism, K2000 have shown a vertical profile of such a balance. The results of experiment C as shown in Fig. 1 (e.g. no relevant deviation from inert

Table 1. *Volume averages of the turbulent Damköhler numbers (1) and the flux Damköhler numbers (2)*

		MS	MF	C
(1)	Da_A	0.6	4.1	6.2
	Da_B	0.8	0.1	2.3
	Da_C	–	–	321
(2)	$Da_{\overline{wa}}$	0.5	3.9	0.4
	$Da_{\overline{wb}}$	3.7	1.7	0.7

shape) and in Table 1 ($Da_{\overline{wa}} = 0.4$) demonstrate that the flux Damköhler number is an appropriate number for estimating the impact of chemistry on vertical reactant flux profiles. Moreover, even if the chemistry is slow with respect to the Damköhler number, the $Da_{\overline{ws}}$ can at the same time have values that are characteristic of moderate chemistry (or the other way round). For example, it is shown in Table 1 that species B is characterised by a Da smaller than one that refers to moderately slow chemical behaviour, i.e. very small deviations from the concentration profile related to the inert case. However, its flux Damköhler number corresponds to fast chemical behaviour (with $Da_{\overline{wb}} = 3.7$ for MS). As a result and as Fig. 2 shows, the flux clearly departs from the inert flux profile.

It is convenient to determine which physical processes are responsible for the vertical profile behaviour
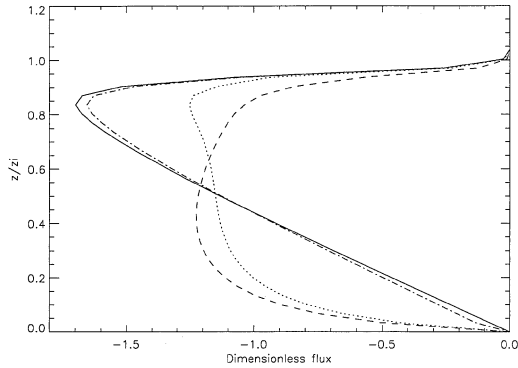

Fig. 2. Vertical profiles of the dimensionless fluxes for the top-down scalar B. The fluxes for the various chemical cases are presented: Inert (solid line), MS (dotted line), MF (dashed line) and C experiments (dash dot line). The values are made dimensionless by $w_* b_*$ for the chemical fluxes where w_* and b_* are the convection velocity scale and the concentration scale for the top-down scalar as defined in eq. (9) respectively.

of the inert scalar flux. All the dynamical terms of eq. (1) have been calculated explicitly in the I experiment. For this case, our results are similar to previous studies [e.g. Cuijpers and Holtslag (1998) and Moeng and Wyngaard (1989)] and therefore the budget of the resolved flux of a bottom-up inert scalar is not shown here. Briefly, for non-reactive fluxes, this budget reveals a balance between on the one hand the gradient and the buoyancy production terms, which are the major flux sources up to the middle of the boundary layer, and on the other hand the pressure and dissipation at smaller scales which tend to destroy the fluxes.

In order to study the relevance of the chemical contribution to the fluxes, we calculated the chemical term, i.e. eq. (5), in the flux budget equations [eq. (1)]. The budget is now analysed for the moderately fast chemical case (MF) for which the effect of chemistry is the most important. Indeed, as expected by analysing the flux profiles, we find that the chemical contribution is negligible for the chemical equilibrium case and small for the moderately slow chemical case. In Fig. 3, the vertical contributions to the flux budget equation (Fig. 3a) and the ratios of the chemical contribution to the dynamical contributions (Fig. 3b) for the MF experiment are presented. In Fig. 3b, since the chemistry acts as a destruction term, the minus ratio has been plotted so that the sign of the ratio is the one of the denominator. Note that all the terms of the flux budget equation have been calculated explicitly. In the lowest part of the boundary layer (i.e. for $z/z_i < 0.1$), the turbulent transport is still the major dissipative contributor to the flux. Nevertheless, in the bulk of the CBL (between 0.1 and $0.8 z/z_i$), the chemistry becomes the dominant sink since its ratios with the pressure term and sub-grid dissipation contributions reveal values larger than 1. From the middle of the boundary layer to the upper part, the chemical term becomes even more important than the gradient or the buoyancy terms (in absolute values).

The buoyancy production, i.e. $(g/\Theta_0)\overline{\theta s_i}$, is the most affected term. Owing to chemistry it becomes the smallest production term in the whole convective boundary layer. Since the heat flux is equal for all the simulations, only the chemistry is responsible for the decrease in the temperature–scalar covariance, i.e. $\overline{\theta s_i}$. To study how the chemistry can affect the buoyancy contribution, we analysed the budget of the covariance between the temperature and the reactant. We find that the chemical term included in the buoyancy budget equation. i.e. $-k(S_i \overline{s_j \theta} + S_j \overline{s_i \theta} + \overline{s_i s_j \theta})$ is a non-negligible dissipative term. In other words,
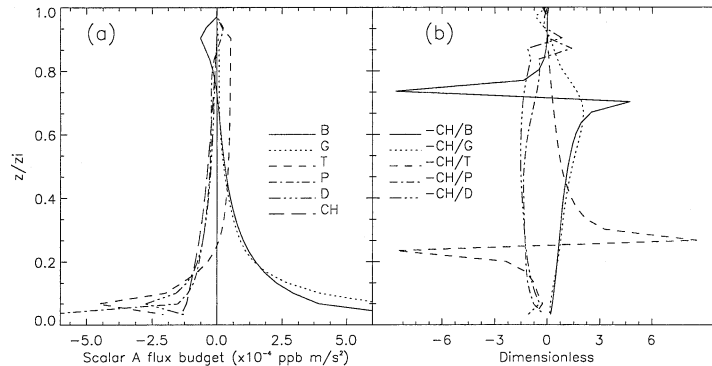
Fig. 3. Vertical profiles of the flux budget equation for the scalar A for the MF case: (a) the contributions to the flux budget equation (B, buoyant production; G, gradient production; T, turbulent transport; P, pressure correlation; D, dissipation; CH, chemistry), (b) the ratios of the chemical term to buoyancy ($-CH/B$), to gradient production ($-CH/G$), to turbulent transport ($-CH/T$), to pressure contribution ($-CH/P$) and to dissipation ($-CH/D$).

when deriving a parameterisation for reacting scalar fluxes, one should pay particular attention first to the treatment of the chemical contribution to the buoyancy contribution, and then to the entire contribution that buoyancy makes to the flux. Hamba (1993) has neglected the chemical term in the buoyant production term, assuming that the buoyancy term is proportional to the temperature and mean scalar concentration gradient. However, Verver (1994) showed that the chemical term is relevant on the governing equation for $\overline{\theta s_i}$. For instance, Verver et al. (1997) proposed, on the basis of budget analysis, a second-order closure model that accounts for the chemistry in flux and buoyancy budget equations.

4. Scalar variances

Figure 4 shows the effect that an increase in the reaction rate can have on the variance bottom-up vertical profiles. Since the maximum scalar flux occurs with the high scalar gradient near the surface, it is the mechanical production of scalar variance which is responsible for the peak values observed in the bottom of the CBL. The inert scalar variance profile shows a secondary maximum around $0.9z_i$ close to the entrainment zone.

For reactive scalars undergoing moderately slow and fast chemistry, the profiles deviate from the inert shape. These deviations are more significant for the moderately fast chemical case (with higher Damköhler numbers, see Table 2). As shown by Sykes et al. (1994), one can notice that even for the moderately slow chem-
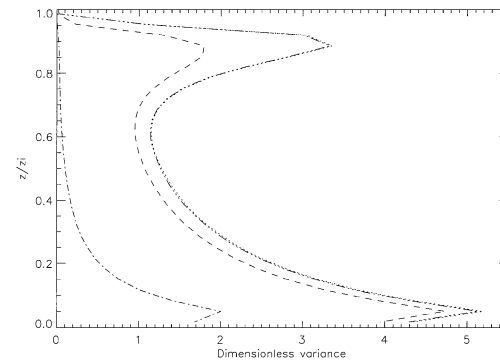

Fig. 4. Vertical profiles of the dimensionless variances for the bottom-up scalar A. The chemical variances for the various chemical cases are plotted: Inert (dotted line), MS (dashed line), MF (dash dot lines) and C (dash dot dot dot lines). All values are normalised by c_{u*}^2.

ical case, i.e. $Da_A = 0.6$, the profile shows deviations. Just as in the case of the bottom-up scalar flux, the chemistry acts as a sink term. The chemical term destroys the variance and additionally limits the vertical penetration of the variance. As a result, the largest deviations for all the simulations occur at the upper part of the CBL.

In Table 2, the volume averages of the Damköhler numbers for (co-)variances, i.e. $Da_{\overline{s^2}}$ and $Da_{\overline{s_i s_j}}$, are reported. The calculation procedure is the same as for Table 1 and uses eqs. (13) and (14). The importance of variance deviations as shown in the figure can be directly related to the $Da_{\overline{s^2}}$, e.g. the largest deviations are reported for the chemical case with the largest

Table 2. *Volume averages of the Damköhler numbers for (co-)variances*

	MS	MF	C
$Da_{\overline{a^2}}$	1	7.7	0.7
$Da_{\overline{b^2}}$	7.2	3.2	0.7
$Da_{\overline{ab}}$	3.3	2.2	0.8

$Da_{\overline{a^2}}$. As indicated by the low value of the Damköhler numbers for both variances in the cycle chemical case ($Da_{\overline{a^2}} = 0.7$ and $Da_{\overline{b^2}} = 0.7$), the profiles obtained for the inert and the cycle are rather similar.

The budget equation of the resolvable-scale inert scalar variance can be derived by taking the dynamical terms of eq. (2) and writing $j = i$. This budget (not shown in the paper) has been compared with the temperature variance budget reported in Fig. 7 of Moeng and Wyngaard (1989). Our results show good agreement with this study except in the upper CBL, where the magnitude of our terms is lower due to the difference between the inert scalar flux and the heat flux in this region (see also Fig. 1). For an emitted scalar, the mean gradient contribution (G) is a source of variance in the whole CBL. However, for temperature, G becomes negative in the mid-CBL due to the entrainment of dry air from the free troposphere (counter-gradient effect).

We studied the relevance of the chemical contribution to the variance by analysing the chemical contribution to the variance budget equations. In Fig. 5 the contributions to the variance budget equation (Fig. 5a) and the ratios of the chemical contribution to the dynamical contributions (Fig. 5b) for the moderately fast chemical case are presented. The minus ratio has been plotted for the same reason as in the case of the fluxes. The chemical contribution is more important than the gradient production (in absolute values) and than the dissipation at smaller scales (around two times larger in the mid-CBL). In the bulk, there is a balance between production by the turbulent transport term and destruction by sub-grid dissipation and chemistry. Since the increase of the chemical rate resulting from the increase of B entrainment flux in the MF experiment, limits the variance penetration, the location of the maximum turbulent transport contribution moves down from the mid-CBL to the low-CBL.

Compared to the chemical contribution to the fluxes which acts as a sink for either the emitted scalar A or for the entrained scalar B, here the chemical term can act as a production or destruction term with respect to A or B variances. Sykes et al. (1994) noticed that increasing the reaction rate produces larger top-down scalar variances and therefore increases the deviations from the inert shape. Since we know that the reactants A and B are anti-correlated, and since we have analysed the chemical contribution [eq. (6)] in all our numerical experiments, we find that the latter is composed of competing terms, one that destroys variances and one that produces variances. For a second-order reaction, the first term (i.e. $-k\overline{a^2}B$ for the emitted scalar) is always negative because the variance and the mean concentration are positive. Since the scalars A and B are always anti-correlated (i.e. $\overline{ab} < 0$), the second term (i.e. $-k\overline{ab}A$ for the emitted scalar) becomes a productive contribution to the variance. The third-order term is small compared to the other terms (Petersen, 2000). For the emitted scalar, the sink chemical term dominates the variance behaviour and as a result causes
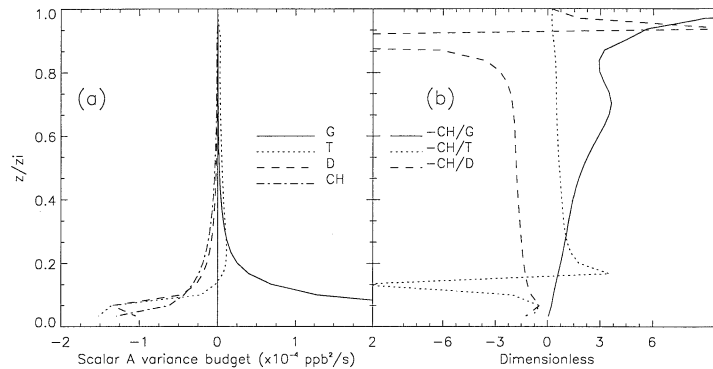

Fig. 5. As Fig. 3 but for the variance budget equation.

a decrease in the dimensionless variance. For the entrained scalar, the variance behaviour is dominated by the production chemical term. Therefore, the increase of the reaction rate generates an increase of the entrained scalar variance.

5. Scalar covariances

The chemical transformations in the CBL depend on the efficiency of reactant mixing. This efficiency is determined by the ability of turbulence to bring the reactants together. In the case of non-premixed reacting scalars, the reaction rate can be slowed down due to heterogeneous mixing. The covariance between reactants, i.e. $\overline{ab}$, is the variable that accounts for the segregation of species in the CBL. It is an explicit term in the governing equation for the mean concentration.

Figure 6 shows the vertical profiles of the resolved concentration fluctuation covariances. For the MS and the MF experiments, the profiles deviate significantly from the inert shape. For the moderately fast chemical case, these deviations are more significant in the upper CBL, whereas the MS covariance profile is affected in almost the entire CBL. As shown in Table 2, the latter profile is the one affected most by chemistry ($Da_{\overline{ab}} = 3.3$). From the turbulent Da [eq. (8)] one might expect the chemical term to have a larger impact in the MF experiment than in the MS
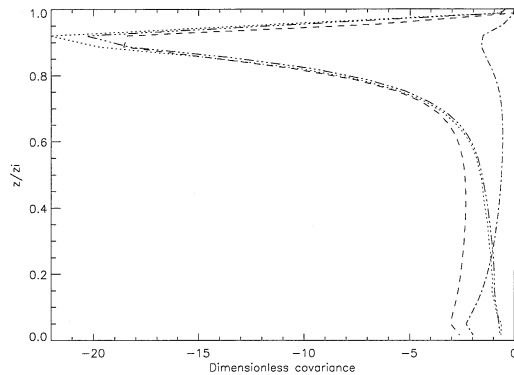

Fig. 6. Vertical profiles of dimensionless reacting scalar covariances. The chemical variances for the various chemical cases are plotted: Inert (dotted line), MS (dashed line), MF (dash dot line) and C experiments (dash dot dot dot line). The values are made dimensionless by $c_{u*}c_{d*}$. The top-down chemical scale, c_{d*}, has been calculated by taking the absolute value of the ratio of the top-down scalar flux in the inert case at z_i to the convective velocity scale w_*.

experiment [$Da_A(MS) = 0.6$ and $Da_A(MF) = 4.1$]. However, as shown in Fig. 6 and due to the large $Da_{\overline{ab}}$ in the bulk of the CBL, the chemical term causes similar deviations from the inert shape in the MS and MF experiments both characterised by $Da_{\overline{ab}} > O(1)$. This indicates that the $Da_{\overline{s_i s_j}}$ are appropriate parameters for estimating the chemical impact on the vertical reactant covariance profiles. Notice that chemistry has different impacts on the profile, depending on the height. For instance in the MS case, the chemistry acts as a sink up to $0.8z_i$ (around $0.3z_i$ for the moderately fast one) and, in the upper CBL, it creates covariance. As shown by the covariance Damköhler number for the C experiment ($Da_{\overline{ab}} = 0.8$), the vertical profile for reactants undergoing a chemical cycle is rather similar to the profile of inert scalars covariance.

Before focusing on the contribution made by the chemical term to the covariance, we describe the budget of the covariance for the inert bottom-up scalar (not shown). The complete budget equation is given in section 2. In view of the fact that we have a negative covariance due to the opposite transport of reactants A and B, we always find that the gradient term acts as a sink in the entire CBL. The turbulent transport acts only as a sink in the upper CBL. Finally, the most noticeable point is that the dissipation term is always a source of covariance, except above $0.9z_i$.

We introduced a chemical term, i.e. eq. (7), into the budget equations in order to study the chemical contribution to covariances. Figure 7 shows the contributions to the covariance budget equation (Fig. 7a) and the ratios between the chemical term of the covariance budget equation and the other contributions to covariances (Fig. 7b) for the MF experiment. The turbulent transport contribution is the one that is affected most by chemistry: it shifts from a productive to a dissipative contribution. The various contributions all have the same order of magnitude in the mid-CBL. Nevertheless in the lower and upper part of the CBL, the gradient contribution is significantly more important than the chemistry term. Notice that the chemical term acts as a source in the main part of the CBL and as a sink near the surface (as the C/G ratio is positive in this region). As we pointed out previously in our discussion of reactant variances, the chemical term in the budget equation [see eq. (7)] is composed of various contributions that have opposite impacts on the covariance behaviour. Since the scalars are always anti-correlated in our experiments, the terms related to the product of the covariance and the mean scalar concentration (i.e. $-k\overline{ab}B$ and $-k\overline{ab}A$) are always positive and
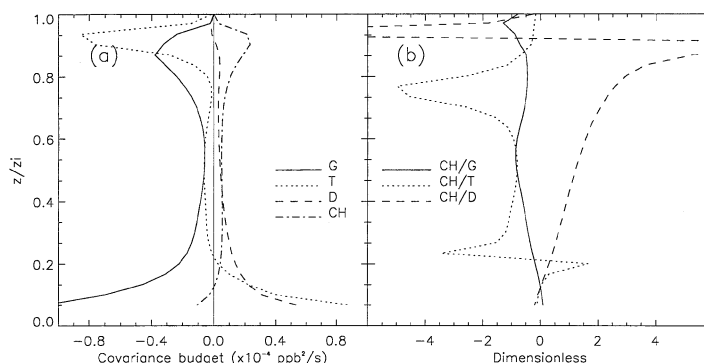
Fig. 7. As Fig. 3 but for the covariance budget equation.

therefore always acts as sources. The variance-containing terms, $-k\overline{a^2}B$ and $-k\overline{b^2}A$, always sinks because the variances are positive. If the chemical term acts as a total sink or source depends on the order of magnitude of the single variance/covariance contributions.

6. Parameterisation for the segregation of the reactants

Here, we derive a parameterisation to account for the segregation of species in a CBL. In the derivation we use the LES results presented previously (1) to account explicitly for the chemical contribution to the (co-)variances and (2) to evaluate the parameterisation. We present the derivation of the parameterisation for reacting scalar transported in opposite directions. In the appendix, we extend it for chemical species transported in the same direction. We first apply the parameterisation to the reacting flows presented previously. Then, the parameterisation is applied to a more complex atmospheric chemical scheme which simulates the formation and the depletion of ozone in the CBL.

6.1. Derivation

An appropriate term for characterising the state of mixing of reactants in the CBL is the vertical profile of the intensity of segregation (I_s), defined as the ratio of the fluctuation reactant concentration covariance to the product of the mean concentrations:

$$I_s = \frac{\overline{ab}}{AB}, \tag{15}$$

where $\overline{ab}$ is the covariance between the reactants and A and B are the averaged concentrations.

Petersen and Holtslag (1999) proposed a parameterisation using a mass-flux approach to represent the asymmetry of the transport in the CBL. They found that their parameterisation, which gives an expression of covariances as a function of turbulent reacting fluxes, is valid for all reacting flows. However, the implementation of their parameterisation in large atmospheric models requires to include the evolution of variables such as the boundary layer depth, the vertical variance velocity and the vertical profiles of the reactant fluxes. These evolution equations are usually not included in large atmospheric models.

In our more simple approach, we derive a parameterisation based on variables that are already calculated by large-scale models. Since the concentration fluctuation covariance is the variable which accounts for the segregation of species, it constitutes the starting point for our derivation. This covariance is related to the correlation coefficient ρ in the following way:

$$\rho = \frac{\overline{ab}}{\sigma_A \sigma_B}, \tag{16}$$

where σ_A and σ_B are the standard deviations of the reactants.

In our LES results, we found that ρ has an almost constant value in the entire CBL for moderately slow and fast chemistry (between -0.6 and -0.8 in both cases). In the case of chemical equilibrium or no chemistry, the value of ρ varies from -0.4 at the bottom of the CBL bulk to -0.9 at the top. Averaging the correlation coefficient over the entire CBL gives $\langle \rho \rangle = -0.75$, where the brackets represent the average over the whole CBL. Measurements from aircraft of NO and O_3 (Vilà-Guerau de Arellano et al., 1993), gave

an average value of around -0.7. By assuming the constant value with depth $\langle \rho \rangle$ to be equal to -0.75 and by combining eqs. (15) and (16), we can write

$$I_{\mathrm{s}} = \langle \rho \rangle \frac{\sigma_{\mathrm{A}} \sigma_{\mathrm{B}}}{AB} = \langle \rho \rangle \frac{(\overline{a^2})^{\frac{1}{2}} (\overline{b^2})^{\frac{1}{2}}}{AB}. \tag{17}$$

The I_{s} calculated using eq. (17) (e.g. with standard deviations and concentrations determined by LES) shows a satisfactory agreement with the one determined by LES where reactant covariances are calculated explicitly e.g. using eq. (15).

Since in a large atmospheric chemical model, the standard deviations σ_{A} and σ_{B} are not calculated explicitly, we derive a more complete expression of eq. (17) where the standard deviations are calculated from variance and covariance functions, as defined by Moeng and Wyngaard (1984). For instance, Wyngaard (1983) showed that every scalar can be written as the sum of a top-down scalar (subscript t) and bottom-up scalar (subscript b). Therefore, the scalar variance can be expressed as

$$\overline{c^2} = \overline{c_{\mathrm{t}}^2} + 2\overline{c_{\mathrm{b}} c_{\mathrm{t}}} + \overline{c_{\mathrm{b}}^2}. \tag{18}$$

Moeng and Wyngaard (1984) decomposed this inert scalar variance into three contributions, i.e.

$$\overline{c^2} = \left(\frac{\overline{wc_{\mathrm{e}}}}{w_*} \right)^2 f_{\mathrm{t}} + 2 \frac{\overline{wc_{\mathrm{e}}} \, \overline{wc_{\mathrm{s}}}}{w_*^2} f_{\mathrm{tb}} + \left(\frac{\overline{wc_{\mathrm{s}}}}{w_*} \right)^2 f_{\mathrm{b}}, \tag{19}$$

where $\overline{wc_{\mathrm{e}}}$ and $\overline{wc_{\mathrm{s}}}$ are the entrainment flux and the surface flux, respectively. The functions f_{t}, f_{b} and f_{tb} are the variance and covariance functions. Moeng and Wyngaard (1984) estimated these functions by fitting their LES results and they obtained the following expressions:

$$f_{\mathrm{t}} = 0.47 \left(\frac{z}{0.9z_i} \right)^{-\frac{5}{4}}, \tag{20}$$

$$f_{\mathrm{b}} = 2.1 \left(1 - \frac{z}{0.9z_i} \right)^{-\frac{3}{2}}, \tag{21}$$

$$f_{\mathrm{tb}} = 1, \tag{22}$$

where $0.9z_i$ accounts for our definition of the boundary layer height which differs from the definition used by Moeng and Wyngaard (1984) (see also Fig. 1). In order to evaluate expression (19), we calculate the vertical profiles of the variances for an inert emitted scalar and an inert entrained one using the expression (19)

together with eqs. (20)–(22). These latter profiles compare with the LES results with a satisfactory agreement (not shown).

Because the inert variance budget equation deals only with dynamical contributions, the functions f_{t} and f_{b} account for dimensionless dynamical contributions to the c_{t} and c_{b} variance budgets. In Figs. 4 and 5 we have shown that the chemical terms can be of the same order of magnitude than the dynamic terms. Therefore we propose to add chemical terms (ch_{t} and ch_{b}) to account for the dimensionless chemical contribution to the variances c_{t}^2 and c_{b}^2. These expressions now read:

$$\overline{c_{\mathrm{t}}^2} = \left(\frac{\overline{wc_{\mathrm{e}}}}{w_*} \right)^2 (f_{\mathrm{t}} + ch_{\mathrm{t}}), \tag{23}$$

$$\overline{c_{\mathrm{b}}^2} = \left(\frac{\overline{wc_{\mathrm{s}}}}{w_*} \right)^2 (f_{\mathrm{b}} + ch_{\mathrm{b}}). \tag{24}$$

In section 2 we deduced the variance Damköhler numbers [see eq. (13)] to classify the reacting flows and to evaluate the relevance of accounting for chemical terms in reactant variance budgets. We showed that these numbers are appropriate parameters for estimating the chemical impact on vertical reactant profiles. Based on these results, we assume that the chemical terms ch_{t} and ch_{b} are related to the variance Damköhler numbers:

$$ch_{\mathrm{t}} \propto Da_{\overline{b^2}}, \tag{25}$$

$$ch_{\mathrm{b}} \propto Da_{\overline{a^2}}, \tag{26}$$

where $Da_{\overline{a^2}}$, $Da_{\overline{b^2}}$ are defined by using eq. (13). Notice that we do not include a correction for f_{tb} because we assume that the chemistry has no effect on this covariance function.

In order to further simplify expressions (25) and (26), we analyse the different components of the terms $Da_{\overline{a^2}}$ and $Da_{\overline{b^2}}$. Since the variance Damköhler numbers are derived from the chemical contribution to the variance budget equations, we analyse the importance of the different components of the chemical term in the variance equation. In section 4 we discussed that the chemical contribution to the variance [eq. (6)] was composed of competing terms. Based on the analysis of these competing terms, we found that one component, i.e. $k\overline{a^2}B$, is the most important term of the bottom-up scalar variance profile behaviour. By using the characteristics scales of a turbulent reacting flow defined in section 2, this term can be made nondimensional as $Da_{\mathrm{A}} \tilde{a}^2$ where $\tilde{a}^2$ is the dimensionless

Table 3. *The averaged value of the intensity of segregation ($\langle I_s \rangle$ averaged between $0.2z_i$ and $0.8z_i$)*

	A + B $\rightleftharpoons$ C			Complex chemistry	
	MS	MF	C	RH and OH	NO_2 and OH
$\langle I_s \rangle$ (LES)	−0.19	−0.21	−0.01	−0.17	−0.05
$\langle I_s \rangle$ (parameterisation)	−0.14	−0.37	−0.01	−0.23	−0.03

variance. Therefore for species that are emitted at the surface we approximate (26) by

$$Da_{\overline{a^2}} \propto Da_A. \tag{27}$$

For species entrained from the free troposphere, the main contribution to the top-down scalar variance profile is the term $-k\overline{ab}B$. Using a similar derivation as for expression (27), we obtain

$$Da_{\overline{b^2}} \propto Da_A \frac{a_* b_*}{b_*^2}, \tag{28}$$

where the concentration scales a_* and b_* are calculated using eq. (9) for inert fluxes.

By substituting the eqs. (23) and (24) for the variances c_t^2 and c_b^2 in eq. (19) and using the approximations (27) and (28), we obtain the following expression for the variance of a reactant emitted at the surface:

$$\overline{a^2} = \left(\frac{\overline{wa_e}}{w_*} \right)^2 \left(f_t + \beta Da_A \frac{a_* b_*}{b_*^2} \right) + 2 \frac{\overline{wa_e}\,\overline{wa_s}}{w_*^2} f_{tb}$$
$$+ \left(\frac{\overline{wa_s}}{w_*} \right)^2 (f_b + \alpha Da_A). \tag{29}$$

A similar expression is found for the variance of a species entrained from the free troposphere:

$$\overline{b^2} = \left(\frac{\overline{wb_e}}{w_*} \right)^2 \left(f_t + \beta Da_A \frac{a_* b_*}{b_*^2} \right), \tag{30}$$

where $\alpha = -0.3$, $\beta = 0.9$ are fitting coefficients determined from the LES simulations. Finally by using the variance expressions (29) and (30) in eq. (17), one can obtain a parameterisation for the intensity of segregation that depends on the mean concentrations, the fluxes at the boundaries and the Damköhler numbers.

6.2. Evaluation

We first evaluate the parameterisation of I_s to the reacting flows presented previously. The validation is

focused on a vertically integrated $\langle I_s \rangle$. We consider that this is the easiest way to introduce the effect of turbulence on chemical reactions on large atmospheric models. Our suggestion is to substitute the chemical reaction rate k by an effective chemical reaction rate k_{eff} where the influence of the turbulent mixing on the chemical transformations is included. This can be written as follows:

$$k_{eff} = k \left(1 + \left\langle \frac{\overline{ab}}{AB} \right\rangle \right) = k(1 + \langle I_s \rangle). \tag{31}$$

Table 3 shows a comparison of vertically integrated parameterised $\langle I_s \rangle$ versus the vertically integrated LES $\langle I_s \rangle$. For the simple chemical pathway, the parameterisation shows good agreement with the LES results even if the parameterised $\langle I_s \rangle$ is overestimated in the MF experiment. These values show that even for moderately slow chemistry, the segregation of reactants plays an important role in chemical transformation. For instance, in the latter case the $\langle I_s \rangle = -0.19$ indicates that the reaction rate is 19% slower that the rate expected when reactants are perfectly mixed. As shown previously, the $\langle I_s \rangle$ for a cycle show a very small value ($\langle I_s \rangle = -0.01$).

We now test our $\langle I_s \rangle$ parameterisation to a mechanism that simulates ozone formation and depletion in the CBL. The chemical mechanism was studied by means of LES by K2000. The chemical mechanism is composed by eleven reactions including two photolytic ones (Table 4). The initial concentration profiles and emission fluxes presented by K2000 are used. We reproduce one of the sensitivity runs with uniform emission of RH and NO and $f = 300$ (see the Table 4 of K2000). Dry deposition is not considered in our simulation leading to some small differences in reactant fluxes close to the surface. Another difference is that in our LES simulations, the entrainment of species is simulated dynamically since our inversion layer evolves with time.

The parameterised vertically integrated $\langle I_s \rangle$ is calculated for this complex mechanism as follows: (1)

Table 4.   *Chemical mechanism used by K2000*[a]

Parameter	Value	Reaction
J_1	2.7×10^{-6}	$O_3 \rightarrow 2OH + O_2$
J_2	8.9×10^{-3}	$NO_2 \rightarrow NO + O_3$
k_1	4.75×10^{-4}	$O_3 + NO \rightarrow NO_2 + O_2$
k_2	6.0×10^{-3}	$OH + CO \rightarrow HO_2 + CO_2$
k_3	$6.0 \times 10^{-3} \times f$	$OH + RH \rightarrow HO_2 + products$
k_4	2.1×10^{-1}	$HO_2 + NO \rightarrow OH + NO_2$
k_5	5.0×10^{-5}	$HO_2 + O_3 \rightarrow OH + 2O_2$
k_6	7.25×10^{-2}	$2HO_2 \rightarrow H_2O_2 + O_2$
k_7	2.75×10^{-1}	$OH + NO_2 \rightarrow HNO_3$
k_8	1.75×10^{-3}	$OH + O_3 \rightarrow HO_2 + O_2$
k_9	2.75	$OH + HO_2 \rightarrow H_2O + O_2$

[a]The reaction rate constants were taken from Stockwell et al. (1990) and Poppe and Lustfeld (1996). Photolysis frequencies and reaction rates are given in s^{-1} and ppb^{-1} s^{-1}, respectively. In our simulation the factor f is set to 300.

Calculation of the Damköhler numbers based on the vertical profile of the concentrations. (2) Calculation of the scales w_*, a_* and b_*. The concentration scales are calculated from the prescribed surface fluxes and the estimated entrainment fluxes. In our case, these latter fluxes are explicitly calculated by LES. In large-scale models, one can approximate them by w_e (c_{CBL} − c_{FT}), where w_e, is the exchange velocity, and c_{CBL} and c_{FT} are the concentrations in the CBL and in the free troposphere. Notice that the concentration scales are calculated using eq. (9) for inert fluxes. Therefore the flux profiles are not needed, they can be directly estimated since the fluxes of inert scalars are linear. (3) Calculation of the variance Damköhler number of the reactants involved in such reactions. For species transported in opposite directions, use eqs. (27) and (28) and for species transported in the same direction see the appendix. (4) Calculation of the parameterised variances with eqs. (29) and (30). (5) Calculation of the vertically integrated $\langle I_s \rangle$ with eq. (17). Notice that by using this procedure one can also obtained vertical profiles of the effective reaction rate.

For this chemical mechanism that simulates the ozone formation and depletion in a CBL, the reaction between RH and OH and the reaction between NO_2 and OH are the ones that give the largest intensity of segregation. Therefore, we apply the new parameterisation to these two reactions. The results show that the bulk parameterisation of $\langle I_s \rangle$ is able to reproduce well the LES $\langle I_s \rangle$ results (Table 3).

7. Summary and conclusions

The effect of chemistry on second-order moments of reactants has been studied by means of large eddy simulation. Four chemical cases that represent different reacting flows and involve an emitted and an entrained reactants have been simulated. We have investigated the relevance of the chemical contribution to second-order moments by calculating the chemical terms in second-order moment budget equations. A detailed analysis of flux and covariance budgets has been carried out and the contribution of chemical term has been discussed with respect to the Damköhler numbers for fluxes and covariances.

The results show that the chemical contribution terms of the respective budget equations strongly affect reactant fluxes and (co-)variances. When the reaction rate is increasing, the deviations of second-order moment profiles from the inert profile are larger. For fluxes, chemistry acts as a sink which leads to deviations from the linear profile that is found for inert species. For variances, the vertical profiles show deviations from the inert profile depending on whether the reactant is transported upwards or downwards: the chemistry term can act as a sink or as a variance source. For covariance, the chemical contribution can also act as a source or a sink. By analysing the budget we notice that the contribution to the flux budget that is most affected by the increase in the reaction rate is the buoyancy term and that the turbulence transport term included in the covariance budget equation shifts from source to sink. When the chemistry is in equilibrium, the chemical term becomes negligible and therefore the flux and (co-)variance profiles are similar to those of inert scalars.

In order to determine the relevance of including the chemical contribution in the calculation of turbulent reacting flows, we derived dimensionless numbers, the so-called Damköhler numbers for fluxes and (co-)variances. These numbers are based on the chemical terms for second-order moment budget equations. We show that for flux and (co-)variance Damköhler numbers larger than one, the contribution of chemical terms to second-order moment profiles is significant.

By means of LES, it is possible to calculate the reactants segregation in the CBL. This variable is always neglected in large atmospheric models and, for certain flows, chemical mechanisms could require a parameterisation for this variable. Based on LES results, we

derived an expression for the intensity of segregation which can be included in large atmospheric chemical models. The parameterisation depends on the reactant mean concentrations, on the correlation coefficient and on the standard deviations. Since standard deviations are difficult to calculate in large-scale models, we developed an expression for the variance of the reactants which explicitly includes the effect of the chemical term. When this reactant variance parameterisation is applied to determine the standard deviation, it provides a satisfactory vertically integrated I_s for the whole set of turbulent reacting flows presented here, i.e. the MS, the MF and the C chemical cases. In addition, we have applied the parameterisation to a more realistic atmospheric chemical mechanism accounting for the formation and the depletion of ozone in the CBL. The comparison with LES results have shown the ability of the parameterisation to estimate the intensity of segregation for more complex chemical schemes.

8. Acknowledgments

9. Appendix

For two species emitted at the surface, we have to introduce small variations of the parameterisation to calculate the vertically integrated $\langle I_s \rangle$. These modifications concern the correlation coefficient ρ and the assumptions made to define the dimensionless chemical contributions ch_t and ch_b introduced in eqs. (23) and (24). As a result, the parameterised variances for reactants both emitted at the surface are:

$$\overline{a^2} = \left(\frac{\overline{wa_e}}{w_*} \right)^2 f_t + 2 \frac{\overline{wa_e}\,\overline{wa_s}}{w_*^2} f_{tb} + \left(\frac{\overline{wa_s}}{w_*} \right)^2$$
$$\times \left[f_b + \alpha \left(Da_A + Da_B \frac{a_* b_*}{a_*^2} \right) \right], \qquad (A1)$$

and

$$\overline{b^2} = \left(\frac{\overline{wb_e}}{w_*} \right)^2 f_t + 2 \frac{\overline{wb_e}\,\overline{wb_s}}{w_*^2} f_{tb} + \left(\frac{\overline{wb_s}}{w_*} \right)^2$$
$$\times \left[f_b + \alpha \left(Da_B + Da_A \frac{a_* b_*}{b_*^2} \right) \right]. \qquad (A2)$$

Based on LES results, we propose a correlation coefficient of $\rho = 0.9$ when applying eq. (17) combined with eqs. (A1) and (A2) to calculate the intensity of segregation between reacting scalars emitted at the surface.

REFERENCES

Bretherton, C. S., MacVean, M. K., Bechtold, P., Chlond, A., Cotton, W. R., Cuxart, J., Cuijpers, H., Khairoutdinov, M., Kosovic, B., Lewellen, D., Moeng, C. H., Sibiesma, P., Stevens, B., Stevens, D. E., Sykes, I. and Wyant, M. C. 1999. An intercomparison of radiatively driven entrainment and turbulence in a smoke cloud, as simulated by different numerical models. *Q. J. R. Meteorol. Soc.,* **125**, 391–423.

Cuijpers, J. W. M. and Duynkerke, P. G. 1993. Large eddy simulations of trade wind with cumulus clouds. *J. Atmos. Sci.* **50**, 3894–3908.

Cuijpers, J. W. M. and Holtslag, A. A. M. 1998. Impact of skewness and nonlocal effects on scalar and buoyancy fluxes in convective boundary layers. *J. Atmos. Sci.* **55**, 151–162.

Deardorff, J. W. 1974. Three-dimensional numerical study of turbulence in an entraining mixed layer. *Boundary Layer Meteorol.* **7**, 199–226.

Deardorff, J. W. 1979. Prediction of convective mixed-layer entrainment for realistic capping inversion structure. *J. Atmos. Sci.* **36**, 424–436.

Gao, W. and Wesely, M. L. 1994. Numerical modelling of the turbulent fluxes of chemically reactive trace gases in the atmospheric boundary layer. *J. Appl. Meteorol.* **33**, 835–847.

Hamba, F. 1993. A modified K model for chemically reactive species in the planetary boundary layer. *J. Geophys. Res.* **98**, 5173–5182.

Herwehe, J. A., McNider, R. T. and Newchurch, M. J. 2000. A numerical study of the effects of large eddies on photochemistry in the convective boundary layer. 14th Symposium on Boundary Layers and Turbulence. American Meteorological Society, 235–238.

Krol, M. C., Molemaker, M. J. and Vilà-Guerau de Arellano, J. 2000. Effects of turbulence and heterogeneous emissions on photochemically active species in the

convective boundary layer. *J. Geophys. Res.* **105**, 6871–6884.

Lenschow, D. H., Wyngaard, J. C. and Pennell, W. T. 1980. Mean-field and second-moment budgets in a baroclinic, convective boundary layer. *J. Atmos. Sci.* **37**, 1313–1326.

McDonald-Butler, E. C., Liljestrand, H. M. and Sepehrnoori, K. 1999. Numerical modeling of dry deposition coupled to 22 photochemical reactions. *Atmos. Environ.* **33**, 1491–1502.

Moeng, C. H. and Wyngaard, J. C. 1984. Statistics of conservative scalars in the convective boundary layer. *J. Atmos. Sci.* **41**, 3161–3169.

Moeng, C.-H. and Wyngaard, J. C. 1989. Evaluation of turbulent transport and dissipation closures in second-order modeling. *J. Atmos. Sci.* **46**, 2311–2330.

Molemaker, M. J. and Vilà-Guerau de Arellano, J. 1998. Turbulent control of chemical reactions in the convective boundary layer. *J. Atmos. Sci.* **55**, 568–579.

Patton, E. G., Davis, K. J., Barth, M. C. and Sullivan, P. P. 2001. Decaying scalars emitted by a forest canopy: a numerical study. *Boundary Layer Meteorol.* **100**, 91–129.

Petersen, A. C. and Holtslag, A. A. M. 1999. A first-order closure for covariances and fluxes of reactive species in the convective boundary layer. *J. Appl. Meteorol.* **38**, 1758–1776.

Petersen, A. C., Beets, C., van Dop, H. and Duynkerke, P. G. 1999. Mass-flux schemes for transport of non-reactive and reactive scalars in the convective boundary layer. *J. Atmos. Sci.* **56**, 37–56.

Petersen, A. C. 2000. The impact of chemistry on flux estimates in the convective boundary layer. *J. Atmos. Sci.* **57**, 3398–3405.

Poppe, D. and Lustfeld, H. 1996. Nonlinearities in the gas phase chemistry of the troposphere: Oscillating concentrations in a simplified mechanism. *J. Geophys. Res.* **101**, 14373–14380.

Schumann, U. 1989. Large-eddy simulation of turbulent diffusion with chemical reactions in the convective boundary layer. *Atmos. Environ.* **23**, 1713–1729.

Siebesma, A. P. and Cuijpers, J. W. M. 1995. Evaluation of parametric assumptions for shallow cumulus convection. *J. Atmos. Sci.* **52**, 650–666.

Stockwell, R. W., Middleton, P., Chang, J. S. and Tang, X. 1990. The second generation regional acid deposition model chemical mechanism for regional air quality modeling. *J. Geophys. Res.* **96**, 16343–16367.

Sykes, R. I., Parker, S. F., Henn, D. S. and Lewellen, W. S. 1994. Turbulent mixing with chemical reactions in the planetary boundary layer. *J. Appl. Meteorol.* **33**, 825–834.

Verver, G. H. L. 1994. Comment on "a modified K model for chemically reactive species in the planetary boundary layer" by Fujihiro Hamba. *J. Geophys. Res.* **99**, 19021–19023.

Verver, G. H. L., van Dop, H. and Holtslag, A. A. M. 1997. Turbulent mixing of reactive gases in the convective boundary layer. *Boundary Layer Meteorol.* **85**, 197–222.

Vilà-Guerau de Arellano, J. and Cuijpers, J. W. M. 2000. The chemistry of a dry cloud: the effects of radiation and turbulence. *J. Atmos. Sci.* **57**, 1573–1584.

Vilà-Guerau de Arellano, J. and Lelieveld, J. 1998. Chemistry in the atmospheric boundary layer. In: *Clear and cloudy boundary layers* (eds. A. A. M. Holtslag and P. G. Duynkerke). Royal Netherlands Academy of Arts and Sciences, Amsterdam, The Netherlands, 267–286.

Vilà-Guerau de Arellano, J., Duynkerke, P. G., Jonker, P. J. and Builtjes, P. J. H. 1993. An observational study on the effects of time and space averaging in photochemical models. *Atmos. Environ.* **27**, 353–362.

Wyngaard, J. C. 1983. Lectures on the planetary boundary layer. In: *Mesoscale meteorology–Theories, observations and models.* NATO ASI Series, D. Reidel, Dordrecht, 603–650.

Wyngaard, J. C. 1985. Structure of the planetary boundary layer and implications for its modeling. *J. Climate Appl. Meteorol.* **24**, 1131–1142.

Wyngaard, J. C. and Brost, R. A. 1984. Top-down and bottom-up diffusion of a scalar in the convective boundary layer. *J. Atmos. Sci.* **41**, 102–112.

Wyngaard, J. C., Pennell, W. T., Lenschow, D. H. and LeMone, M. A. 1978. The temperature-humidity covariance budget in the convective boundary layer. *J. Atmos. Sci.* **35**, 47–58.